# Optimization of sliding-vane expanders for a low-enthalpy ORC energy recovery system



IOP Conf. Series: Materials Science and Engineering **604** (2019) 012042 doi:10.1088/1757-899X/604/1/012042

# Optimization of sliding-vane expanders for a low-enthalpy ORC energy recovery system

**Stefano Murgia[1,*], Gianluca Valenti[2], Ida Costanzo[1], Pasquale Pio Manfreda[2]**

[1]Ing. Enea Mattei S.p.A., Italy
[2]Politecnico di Milano, Italy

*stefano_murgia@mattei.it

**Abstract.** Increasingly numerous are the experimental activities on low-grade ORC focused on expanders optimization, in order to increase the cycle net power and efficiency. In the range of small power ORCs, positive displacement expanders are more suitable than dynamic expanders thanks to lower speed, good off-design performance, high expansion ratio, low cost and simple manufacturing. This paper presents an extensive experimental analysis on a low-enthalpy ORC-based recovery system tested in different conditions: two different working fluids (R236fa and R1233zd) and two different sliding-vane expanders (ExpA and ExpB) are tested and the ORC performance are mapped in detail. A particular focus is dedicated to expander optimization: the operating conditions are deeply investigated by using piezoelectric pressure transducers to determine the expansion indicated diagram and the expander mechanical efficiency. Also the effect of the variation of both the expander and pump rotational speeds is investigated. The thermal source is the hot lubricant of a mid-size air compressor, the thermal sink is tap water.

## 1. Introduction

A large amount of the total waste thermal energy is dissipated as low-enthalpy thermal source (30°C-200°C). The most widely used solution to take advantage of these low-enthalpy thermal sources is the Organic Rankine Cycle (ORC). Low-enthalpy waste heat can also come from equipment such as compressors, where the lubricating oil circuit is continuously cooled by ambient air blown by a fan. In compressed air applications, the energy produced by the recovery system could be used directly in the package (i.e. to feed the compressor and its electrical auxiliary) or it could be delivered to the electric grid, in compliance with the local policy. The key elements of ORC design are the choice of the working fluid and of the expander. The choice of the working fluid is critical due to the influence on system efficiency, components sizes, stability and safety. Different studies in literature focus on the definition of a working fluid selection criterion. A review of those criteria has been made by Bao and Zhao [1], highlighting the working fluid physical properties that must be taken into account. Among them saturation curve shape, molecular complexity, critical temperature, vaporization latent heat, density are the most important. Therefore, there are several aspects to consider and different methods to evaluate them, but most of all the working fluid choice is strictly related to heat source thermal level [2]. Another critical aspect is the selection of the expander. In the range of small power ORCs, positive displacement expanders are more suitable then dynamic expanders due to the following features: lower speed, good off-design performance, high expansion ratio, low cost, simple manufacturing [3]. The authors deeply investigated ORC equipped with sliding-vane expanders and pump in previous work [4,5]. The main objectives of this work is the assessment of the performance of an ORC plant and the mechanical and fluid dynamic optimization of a sliding-vane expander. The experimental campaign is carried out on a

small scale 3kW unit in regenerative configuration. One sliding-vane expander in two configurations (ExpA and ExpB) and two different working fluids (R236fa and R1233zd) are used in the test rig. The low-grade thermal source is the lubricant of a sliding-vane air compressor. The next sections describe the experimental method, with a focus on the test rig and the experimental procedure, then results and discussion, conclusions and, ultimately, the future development of the project.

## 2. Experimental method

### *2.1. The test rig*

The power plant consists of a regenerative ORC cycle exploiting lubricating oil, coming from a big size compressor, as heat source. The compression process increases oil temperature which is then typically air-cooled in a radiator. Exploiting this oil as a thermal source in an ORC, it is possible to recover heat that would have been dissipated. The power plant schematic is presented in Figure 1 and is composed by:

- a sliding-vane pump, equipped with a brushless electric motor in order to vary the rotational speed;
- three counter current plates heat exchangers used as evaporator, condenser and regenerator respectively;
- an expansion vessel placed upstream the pump to avoid its cavitation;
- a sliding-vane expander, equipped with a torque meter and an inverter, in order to vary the rotational speed.

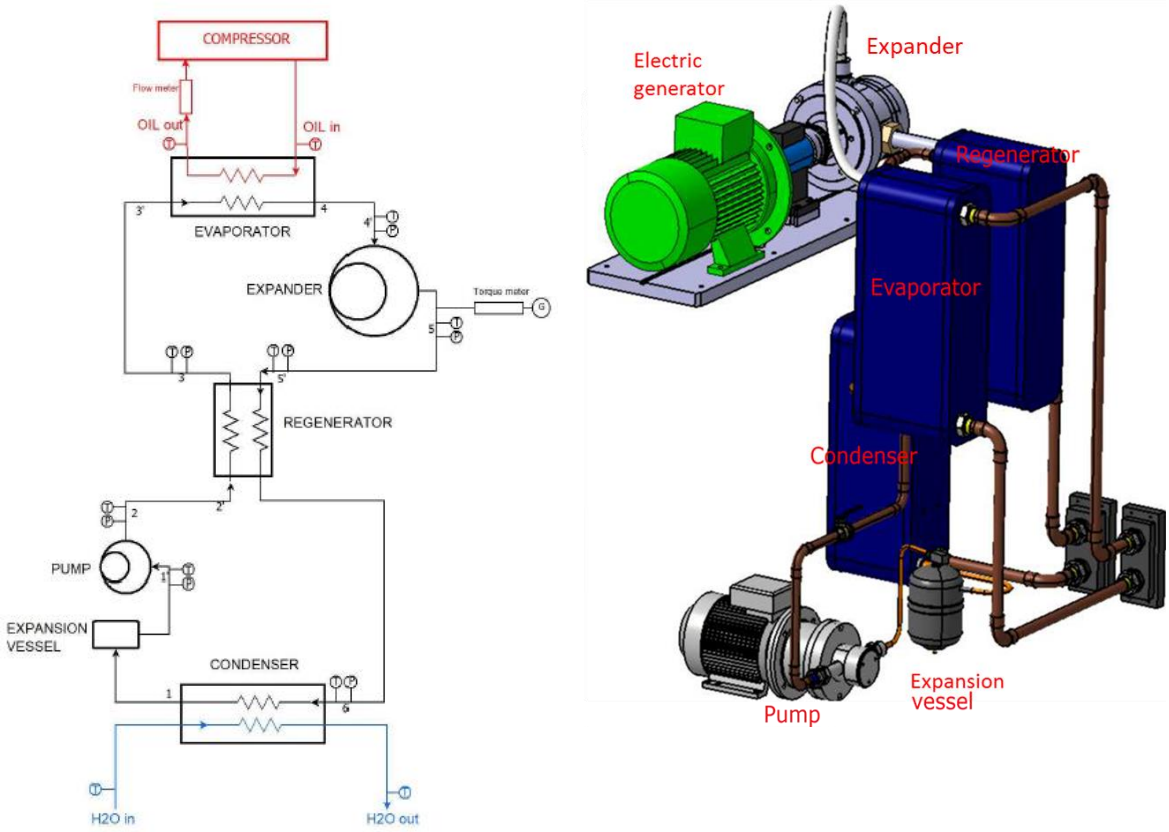


**Figure 1.** ORC cycle in regenerative configuration schematic

One expander in two configurations (ExpA and ExpB) and two different working fluids (R236fa and R1233zd) are used in the test rig. The first part of the experimental campaign is focused on expander optimization. At first, the expander axial gap has been designed according to the maximum value recommended for this machines (ExpA). This parameter affects strongly the volumetric efficiency of the expander: the higher is the axial gap, the higher the machine is in safe condition with respect to any

contact between the rotor and the stator but the higher are the gas leakages through the end-covers. For this reason, in order to optimize the machine, the axial gap has been reduced (-70%) and blades have been modified by increasing the semi-holes thickness (+20%) to allow for a better volumetric efficiency and blades stability. Furthermore, the effect of the variation of the expander rotational speed on the cycle performance has been investigated. The optimized ExpB is then used to compare the ORC performance using two different working fluids: R236fa and R1233zd. The working fluids properties are listed in Table 1. The expanders main geometrical features are listed in **Table** 2.

**Table 1.** Working fluids properties.

| | **R236fa** | **R1233zd** | **Unit** |
|---|---|---|---|
| $MM$ | 152.04 | 130.5 | kg/kmol |
| $T_{cr}$ | 124.92 | 165.6 | °C |
| $P_{cr}$ | 32 | 35.72 | bar |
| $Cp_{liq}$ | 1.21 | 1.24 | kJ/kg K |
| $GWP$ | 9810 | 1 | - |

**Table 2.** Expander geometrical features.

| **Parameter** | **Value** | **Unit** |
|---|---|---|
| $D_{stator}$ | 118.6 | mm |
| $D_{stator}$ | 100 | mm |
| $L$ | 100 | mm |
| $\beta_{volumes}$ | 3.38 | - |

In order to evaluate the thermodynamic conditions of every significant point of the cycle, type T thermocouples and pressure transducers are installed on the test bench. The compressor oil flow rate is measured through a flow meter: this operating parameter allows to determine the thermal power exchanged in the evaporator. The mechanical power of the expander is measured by means of a torque meter. Four piezoelectric pressure transducers are placed on the end cover of the expander; they allow to deeply investigate the expansion process by reconstructing the indicated cycle. Instrumentation uncertainties are listed in **Table** 3.

**Table 3.** Instrument list for the test.

| **Instrument** | **Measured quantity** | **Absolute uncertainty** |
|---|---|---|
| Thermocouple | Temperature | 0.5 °C |
| Pressure transducer | Pressure | 4000 Pa |
| Piezoelectric pressure transducer | Pressure | - |
| Flow meter | Volume flow rate | 5 l min$^{-1}$ |
| Torque meter | Torque, rotational speed | 0.1 Nm, 13 rpm |

### *2.2. Experimental procedure*

The test rig permits to compute all the physical properties needed to reconstruct the thermodynamic cycle. The thermodynamic properties are computed exploiting the NIST Refprop 9.1. The cycle thermal input power, $\dot{Q}_{evap}$ [kW], is computed by the energy balance at the evaporator:

$$\dot{Q}_{evap} = \rho_{oil} \cdot \dot{V}_{oil} \cdot c_{p,oil} \cdot \left(T_{oil,in} - T_{oil,out}\right) \tag{1}$$

where $\rho_{oil}$ [kg/m3] is the oil density and $c_{p,oil}$ [kJ/kgK] is the oil specific heat. These properties are assumed constant because of the small variation of the oil temperature (maximum 20 °C). $\dot{V}_{oil}$ [m3/s] is the oil volume flow rate while $T_{oil,in}$ [K] and $T_{oil,out}$ [K] are the oil temperature at the inlet and outlet of the evaporator respectively. Then the working fluid mass flow rate $\dot{m}_{evap}$ [kg/s] is calculated, according to the energy balance on the evaporator:

$$\dot{m}_{evap} = \frac{\dot{Q}_{evap}}{\left(h_{WF,evap,out} - h_{WF,evap,in}\right)} \tag{2}$$

where $h_{WF,evap,out}$ [kJ/kg] and $h_{WF,evap,in}$ [kJ/kg] are the working fluid enthalpy at the inlet and outlet of the evaporator respectively. The expander filling factor $FF$ [-] can be calculated as:

$$FF = \frac{\rho_{in,exp}\, V_{in,exp}\, n_{exp}\, \omega_{exp}}{\dot{m}_{evap}} \tag{3}$$

where $\rho_{in,exp}$ [kg/m3] is the fluid density at the inlet of the expander, $V_{in,exp}$ [m3] is the volume of the first closed expansion chamber, $n_{exp}$ [chamber] is the number of the expansion chambers in the expander and $\omega_{exp}$ [rpm] is the expander shaft rotational speed. Considering that the evaporating pressure is the pressure at the inlet of the expander, it is possible to relate this parameter to both the expander and pump operating condition, according to the following equation:

$$p_{evap} = R_g \, \rho_{in,pump} \, \frac{V_{in,pump}}{V_{in,exp}} \frac{n_{pump}}{n_{exp}} \, T_{in,exp} \frac{\omega_{pump}}{\omega_{exp}} \tag{4}$$

Thanks to the energy balance at the expander, pump and condenser, the powers are computed respectively as:

$$\dot{P}_{exp,hydr} = \dot{m}_{evap} \, (h_{in,exp} - h_{out,exp}) \tag{5}$$

$$\dot{P}_{pump,hydr} = \dot{m}_{evap} \, (h_{in,pump} - h_{out,pump}) \tag{6}$$

$$\dot{Q}_{cond} = \dot{m}_{evap} \, (h_{in,cond} - h_{out,cond}) \tag{7}$$

where $\dot{P}_{exp,hydr}$ [kW] and $\dot{P}_{pump,hydr}$[kW] are the expander and pump hydraulic powers and $\dot{Q}_{cond}$ [kW] is the thermal power exchanged at the condenser. The expander isentropic efficiency $\eta_{is,exp}$ [-] is calculated as follows:

$$\eta_{is,exp} = \frac{h_{in,exp} - h_{out,exp}}{h_{in,exp} - h_{out,exp,is}} \tag{8}$$

where $h_{out,exp,is}$ [kJ/kg K] is the working fluid enthalpy, calculated considering an isentropic expansion process. The torque meter used on the test measures the mechanical power $\dot{P}_{exp,mech}$ [kW], which is equal to the mechanical power minus the friction losses in the equipment:

$$\dot{P}_{exp,mech} = C_{shaft} \, \omega_{exp} \, \frac{2\pi}{60} = \dot{P}_{exp,hydr} - \dot{P}_{exp,loss} \tag{9}$$

where $C_{shaft}$ [Nm] is the shaft torque, $\omega_{exp}$ [rpm] is the shaft rotational speed. The $\dot{P}_{exp,loss}$ [kW] is the power lost due to the contact between metal parts of the equipment, particularly stator-rotor contact, rotor-vanes and the friction of the bearing system. The $\dot{P}_{pump,mech}$ [kW] instead, is computed with the following equation:

$$\dot{P}_{pump,mech} = I_{pump} \, \omega_{pump} \, \frac{2\pi}{60} \, k_t \tag{10}$$

where $I_{pump}$ [A] is the pump electric motor current density, $\omega_{pump}$ [rpm] is the shaft rotational speed and $k_t$ [Nm/A] is the electrical motor torque constant. Then, the cycle net power $\dot{P}_{mech,net}$ [kW] and the first law mechanical efficiency $\eta_{I,mech}$ [-] are calculated as follows:

$$\dot{P}_{mech,net} = \dot{P}_{exp,mech} - \dot{P}_{pump,mech} \tag{11}$$

$$\eta_{I,mech} = \frac{\dot{P}_{mech,net}}{\dot{Q}_{evap}} \tag{12}$$

An exergy analysis is carried out in order to evaluate the irreversible losses produced by each component and the second law efficiency. The exergy balance on each component is defined as:

$$ex = h - T_0 \, s \tag{13}$$

where $T_0$ [K] is the reference temperature of 293 K and $s$ [J/kg k] is the entropy. In the following equations, the destruction exergy $\dot{E}x_d$ [J/kg], which represents the destructed work for each equipment, is computed.

$$\dot{E}x_{d,exp} = \dot{m}_{evap}\left(\Delta h_{exp} - T_0 \Delta s_{exp}\right) - \dot{P}_{exp,mech} \tag{14}$$

$$\dot{E}x_{d,pump} = \dot{m}_{evap}\left(\Delta h_{pump} - T_0 \Delta s_{pump}\right) - \dot{P}_{pump,mech} \tag{15}$$

$$\dot{E}x_{d,evap} = \dot{Q}_{evap}\left(1 - \frac{T_0}{T_{ml}}\right) - \dot{m}_{evap}\left(\Delta h_{evap} - T_0 \Delta s_{evap}\right) \tag{16}$$

$$\dot{E}x_{d,reg} = T_0\, \dot{Q}_{reg}\left(\frac{1}{\frac{T_{reg,hot,in} - T_{reg,hot,out}}{log\frac{T_{reg,hot,in}}{T_{reg,hot,out}}}} - \frac{1}{\frac{T_{reg,cold,in} - T_{reg,cold,out}}{log\frac{T_{reg,cold,in}}{T_{reg,cold,out}}}}\right) \tag{17}$$

$$\dot{E}x_{d,cond} = \dot{m}_{evap}\left(\Delta h_{cond} - T_0 \Delta s_{cond}\right) \tag{18}$$

The total exergy destructed $\dot{E}x_{d,TOT}$ [J/kg] is thus:

$$\dot{E}x_{d,TOT} = \dot{E}x_{d,exp} + \dot{E}x_{d,pump} + \dot{E}x_{d,evap} + \dot{E}x_{d,reg} + \dot{E}x_{d,cond} \tag{19}$$

The second law mechanical efficiency $\eta_{II,mech}$ [-] is:

$$\eta_{II,mech} = \frac{\dot{P}_{mech,net}}{\dot{P}_{mech,net} + \dot{E}x_{d,TOT}} \tag{20}$$

Comparing the $\dot{E}x_d$ of each component with the total $\dot{E}x_{d,TOT}$ it is possible to evaluate which device has the major loss.

### *2.3. Indicated cycle reconstruction*

The indicated cycle is defined by averaging several consecutive cycles, whose reconstruction is based on piezoelectric transducers angular position on expander cover plate and pressure levels at inlet and outlet ports. Once the indicated cycle is reconstructed, it is possible to compute the indicated specific work $l_{ind}$ [J/chamber round] as:

$$l_{ind} = \int_{V_{min}}^{V_{max}} P\, dV + P_{suction}\, V_{min} - P_{discharge}\, V_{max} \tag{21}$$

and the indicated power as:

$$\dot{P}_{ind} = l_{ind}\frac{\omega_{exp}}{60}\, n_{exp} \tag{22}$$

Finally, it is possible to calculate the expander mechanical efficiency $\eta_{mech,exp}$ [-] as:

$$\eta_{mech,exp} = \frac{\dot{P}_{ind}}{\dot{P}_{mech,net}} \tag{23}$$

## 3. Results and discussion

Results of the expander optimization are presented comparing the results obtained with both ExpA and and ExpB. In Figure 2, it is plotted the evaporating pressure $\boldsymbol{p_{evap}}$ with respect to $\boldsymbol{T_{in,exp}\frac{\omega_{pump}}{\omega_{exp}}}$. According to Equation (4), these two parameters are directly proportional except for the volumetric efficiency of pump and expander. It is possible to see how, at fixed value of abscissa, $\boldsymbol{p_{evap}}$ increases passing from a maximum value of 11.3 bar to 12.4 bar in the new configuration. This is due to the fact

that the leakages decrease, by decreasing the axial gap. An increasing of $p_{evap}$ leads to a growth of the first law efficiency of the cycle, because the ORC better approaches the heat source.

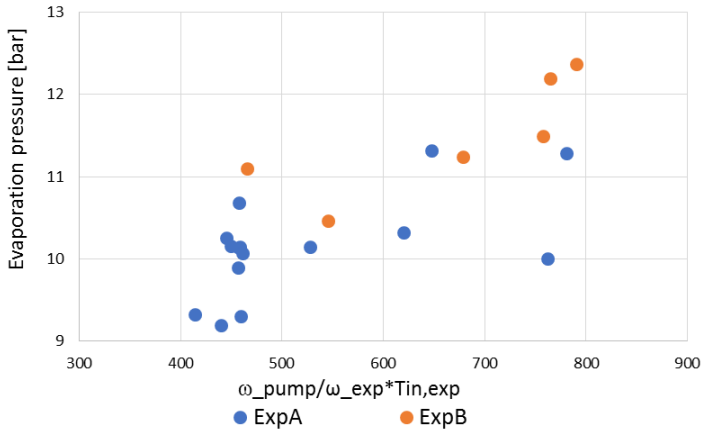


**Figure 2.** Evaporating pressure with respect to rotational speeds for ExpA and ExpB

In Figure 3 instead, it is possible to notice how the $\dot{P}_{exp,mech}$ increases between the two configurations at given mass flow rate. Thanks to lower leakages in ExpB, the flow rate participating to the expansion process is higher and so it is the expander mechanical power.

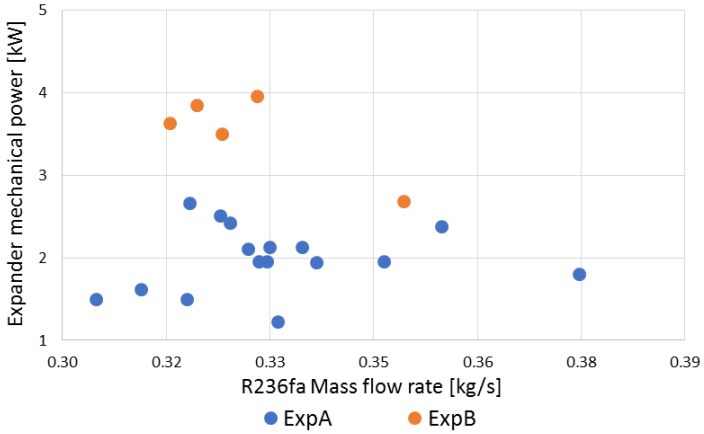


**Figure 3.** Expander mechanical power with respect to working fluid flow rate for ExpA and ExpB

The optimized ExpB is then used to compare the ORC performance using two different working fluids: R236fa and R1233zd. In Figure 4 it is plotted the evaporating pressure with respect to the condensing pressure for both the fluids. The two fluids, working with same heating source, have different working pressures.

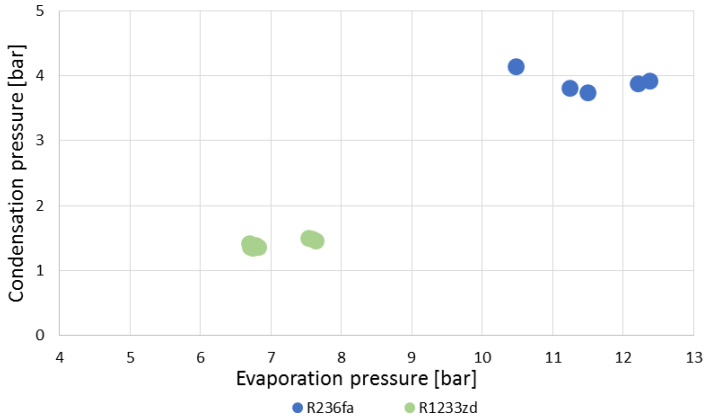


**Figure 4.** Evaporating pressure with respect to condensing pressure for R236fa and R1233zd fluids

In Figure 5, $\boldsymbol{p_{evap}}$ with respect to $\boldsymbol{T_{in,exp}}\frac{\boldsymbol{\omega_{pump}}}{\boldsymbol{\omega_{exp}}}$ using ExpB is presented. These two parameters, help in understanding how the rotational speeds of expander and pump affect the evaporating pressure. It is evident a seemingly proportionality of the two parameters for R236fa whereas it completely mismatches for R1233zd for which the evaporating pressure remains almost constant. This is due to:

- the $\boldsymbol{FF_{exp}}$ is almost constant for the first fluid while it is not for the second. In particular Figure 6, which reports the $\boldsymbol{FF_{exp}}$ against the expander pressure ratio $\boldsymbol{\beta_{exp}}$ shows how it increases with $\boldsymbol{\omega_{exp}}$ in case of R1233zd
- the pump volumetric efficiency $\boldsymbol{\eta_{vol,pump}}$ is not constant

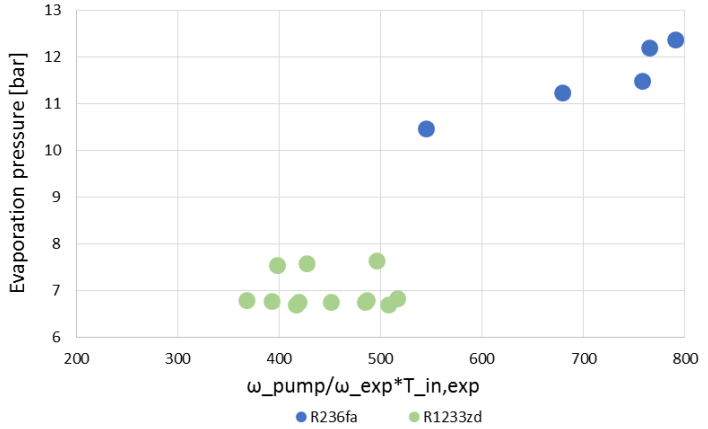


**Figure 5.** Evaporating pressure with respect to rotational speeds with ExpB

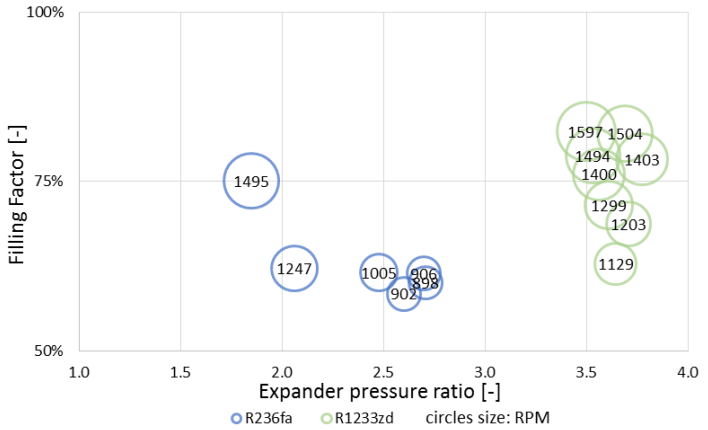


**Figure 6.** Expander filling factor with respect to expander pressure ratio with ExpB

The overall experimental campaign has been carried out considering only one size of heat exchanger for the evaporator. In Figure 7, it is plotted the $\dot{Q}_{evap}$ with respect to the $\Delta T_{PinchPoint}$, with the size of the bubbles representing the expander mechanical power output. The evaporator heat exchanger works as economizer, evaporator and superheating, so it is not possible to define a $\Delta T\_ml$ and as estimation parameter $\Delta T_{PinchPoint}$ is chosen.

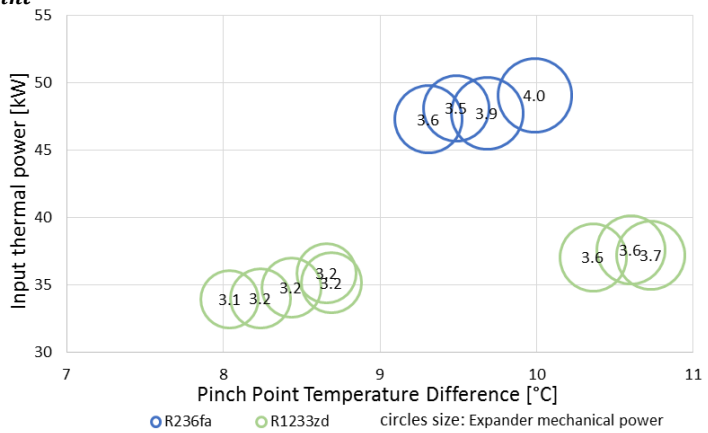


**Figure 7.** Heat exchanged at the evaporator with respect to the pinch point delta temperature

The Figure 7 suggests the following observations:

- for both fluids, as the $\Delta T_{PinchPoint}$ increases, the exchanged heat grows;
- using R236fa there is a larger amount of heating power exchanged at the evaporator. This suggests that this fluid has better exchanging heat property. A plant employing R236fa rather than R1233zd would need smaller heat exchangers and so would cost less;
- for fluid R1233zd, the right-hand side values are reached with a slightly higher temperature of oil (105 against 95 °C). These values see an increasing of entering heat of 12% and a growth of useful power of 16% which translates in an increasing of efficiency of 3%. This is due to the fact that, even if the $\Delta T_{PinchPoint}$ gets higher, the $p_{evap}$ increases and so the $\eta_I$ does.

Moreover, from the Figure 7 it is possible to notice that the two fluids have a difference in entering power of about 30% while the power difference is just 8%. This is a strong proof that the actual ExpB expander is working better with R1233zd. The reason of this, is to be searched in the volumetric behaviour of fluids and expander rotational speed. R1233zd has a volumetric ratio which perfectly matches with that of the expander and a change in expander rotational speed has no effects on the pressures but just on the $FF$ as it is shown in Figure 6. Increasing expander rotational speed can be just beneficial for the indicated power while the mechanical power can feel the effect of increasing friction. R236fa, instead, gets huge benefits by changing $\omega_{exp}$. As it is shown in Figure 6, from 1250 to 1000 rpm the $FF$ stays almost constant whereas the $\beta_{exp}$ increases. If from one side there is a slightly decrease of the flow participating to the expansion, from the other side there is a deep improvement in the expansion process. As well shown in Figure 8, lowering expander rotational speed the recompression, that is highly undesired, is avoided. These results suggest that:

- if the expander has proper dimension for its application a variation of rotational speed can be considered ineffective for the evaporating pressure in fact, despite of really small clearances, the flow leaks;
- if the expander is bigger than the needed application a reduction of $\omega_{exp}$ can have beneficial effect on the thermodynamic of the cycle and on the expansion process;
- it is much better undersizing the volumetric ratio of the expander instead of oversizing it, to not occur in the issue of recompressions.

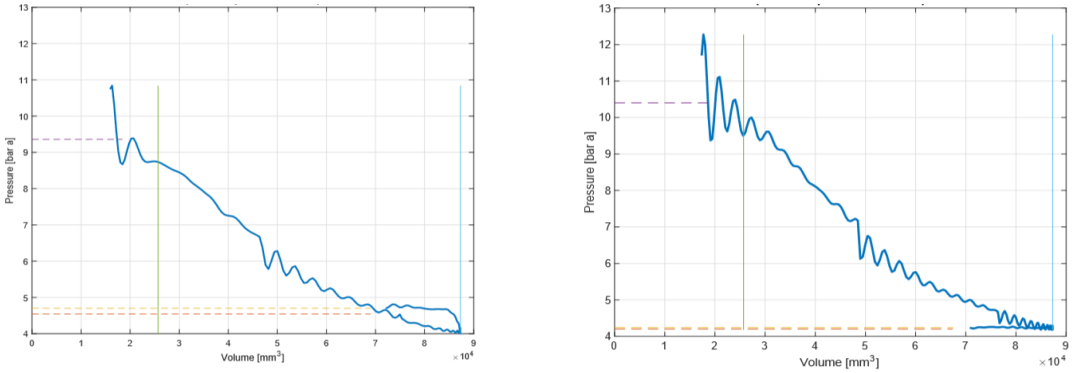


(a) $\omega_{exp} = 1250$ [rpm] (b) $\omega_{exp} = 1000$ [rpm]

**Figure 8.** Indicated diagram using R236fa and ExpB at different rotational speed

Finally, the indicated diagram of the tests with highest mechanical power for both fluids are shown in Figure 9. In both cases, the volumetric ratio of fluids matches that of the machine and this is the main reason way it was possible to reach the highest value of gross mechanical power.

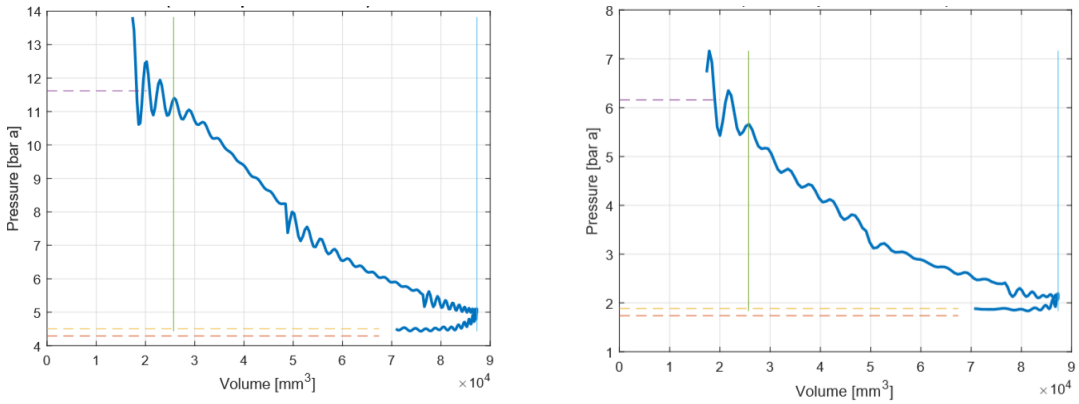


(a) R236fa with $\omega_{exp} = 900$ [rpm] (b) R1233zd with $\omega_{exp} = 1500$ [rpm]

**Figure 9.** Indicated diagram of the test with highest expander mechanical power for the two fluids

For these tests, in **Table** 4 the most important results of the exergetic and energetic analysis are reported. In Figure 10 the pie chart of the loss for each equipment weighted on the total exergetic loss is presented. There is a high percentage of exergy destroyed in the condenser (LTHE), especially with R236fa working fluid. This parameter, because of the low temperature should be negligible, but this is not the case because of the huge fluid sub-cooling undergoes in the condenser (25 °C). This is also one of the reasons why the test with R1233zd has a higher second law efficiency but the most important reason is the fact that with this fluid there is an averagely higher temperature of the heating source. This part of the experimental campaign suggests that R236fa has better heat exchanging properties which allow for smaller heat exchanger. On the other hand, R1233zd allows to work with safer operating conditions thanks to the lower pressures in the plant.

**Table 4.** First and second law analysis in the best cases

| | **R236fa** | **R1233zd** | **Unit** |
|---|---|---|---|
| $\dot{P}_{mech,net}$ | 3.1 | 2.8 | kW |
| $\dot{Q}_{evap}$ | 49.6 | 35.4 | kW |
| $p_{evap}$ | 11.5 | 6.77 | bar |
| $\omega_{exp}$ | 900 | 1500 | rpm |
| $\dot{E}x_{d,TOT}$ | 6.1 | 3.7 | kW |
| $\eta_{I,mech}$ | 6.2% | 7.9% | - |
| $\eta_{II,mech}$ | 33.6% | 42.8% | - |

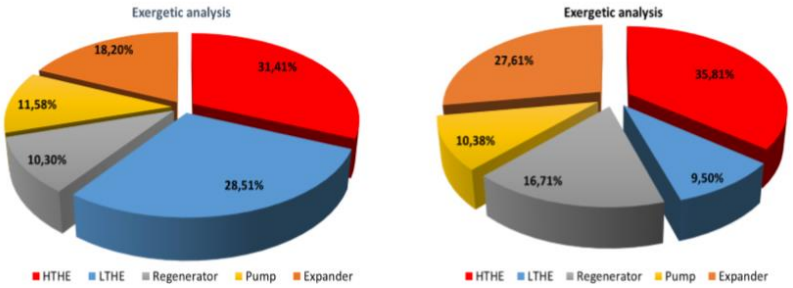


(a) R236fa (b) R1233zd

**Figure 10.** Exergetic analysis

## 4. Conclusions

This work presents the assessment of the performance of an ORC plant as well as on the mechanical and fluid dynamic optimization of sliding-vane expanders. One sliding-vane expander in two configurations (ExpA and ExpB) and two different working fluids (R236fa and R1233zd) are used in the test rig. ExpB compared with ExpA has a reduced the axial gap (-70%) and blades with higher semi-holes thickness (+20%). The optimized ExpB is used to compare the ORC performance using two different working fluids (R236fa and R1233zd). The low-grade thermal source is the lubricant of a sliding-vane air compressor. This work draws the following conclusions.

- ExpB allows to reach higher evaporating pressures and expander mechanical power compared with ExpA. This is basically due to the lower leakages in the machine and to the better blades stability.
- For both fluids, as the minimum temperature difference within the evaporator increases, the input thermal power grows
- R236fa has better heat exchanging properties which allow for smaller heat exchanger. On the other hand, R1233zd allows to work with safer operating conditions thanks to the lower pressures in the plant (-50%)
- The two fluids have a diff erence in input thermal power of about 30% while the mechanical power diff erence is just 8%. This proofs clearly that the actual ExpB expander is working better with R1233zd
- The best case is obtained using ExpB with R1233zd, reaching a first law efficiency of 7.8%
- The best second law efficiency is reached with R1233zd, reaching 42.8%

## References

[1] Bao J, Zhao L, 2013 A review of working fluid and expander selections for organic Rankine cycle, Renewable and Sustainable Energy Reviews 24, 325-342
[2] Wang D, Ling X, Peng H, Tao L 2013 Efficiency and optimal performance evaluation of organic Rankine cycle for low grade waste heat power generation, Energy 50(1), 343–352
[3] Badr O, O'Callaghan P.W, Hussein M, Probert S.D 1984 Multi-vane expanders as prime movers for low-grade energy organic Rankine-cycle engines, Applied Energy 16 (2), 129-146
[4] Murgia S, Colletta D, Costanzo I, Contaldi G 2016 Experimental investigation on ORC-based low-grade energy recovery systems using Sliding-Vane Rotary Expanders, 3rd International Rotating Equipment Conference
[5] Murgia S, Valenti G, Colletta D, Costanzo I, Contaldi G 2017 Experimental investigation into an ORC-based low-grade energy recovery system equipped with sliding-vane expander using hot oil from an air compressor as thermal source, Energy procedia 129C, 339-346